



ELSEVIER

Ultramicroscopy 71 (1998) 257–262

ultramicroscopy

Polarization effect in scanning near-field optic/atomic-force microscopy (SNOM/AFM)

Kunio Nakajima^{a,*}, Yasuyuki Mitsuoka^a, Norio Chiba^a, Hiroshi Muramatsu^a,
Tatsuaki Ataka^a, Katsuaki Sato^b, Masamichi Fujihira^c

^a Technology Center, Seiko Instruments Inc., 563 Takatsuka-shinden, Matsudo, Chiba 271, Japan

^b Faculty of Technology, Tokyo University of Agriculture and Technology, 2-24-16 Nakacho, Koganei, Tokyo 184, Japan

^c Department of Biomolecular Engineering, Tokyo Institute of Technology, Nagatsuta, Midori-ku, Yokohama 227, Japan

Abstract

The polarization effect is reported using a bent optical fiber probe for a scanning near-field optic/atomic-force microscope (SNOM/AFM). We have demonstrated that the SNOM/AFM could be applied to the observation of magnetic domains by imaging polarization contrast in transmission mode. An optical fiber probe with a subwavelength aperture is bent and vibrated vertically as a cantilever for an atomic-force microscope (AFM) for atomic-force regulation. Plane polarized light with an extinction ratio of better than 70 : 1 was emitted by the aperture of the bent probe by controlling the polarization properties of incident light to the probe. By detecting a particular transverse polarization component of light transmitting a sample selected by a polarization analyzer, we obtained clear polarization contrast images of 0.7 μm length bits written on a bismuth-substituted dysprosium-iron-garnet film. © 1998 Elsevier Science B.V. All rights reserved.

Keywords: Polarization contrast; Faraday effect; Magneto-optical film; Optical fiber probe

1. Introduction

There is an ever increasing necessity for tools to investigate the optical properties of materials at the nanometric level. In scanning near-field optical microscopy (SNOM) [1–6], high resolution beyond the diffraction limit has been realized by placing a subwavelength aperture in the proximity of the

sample. This SNOM technique mainly uses the shear-force feedback of vibrating the straight-probe laterally on the sample surface to control the tip-sample separation. In another study, a bent micropipette was proposed as a cantilever in the contact mode [7]. We have already developed a SNOM/AFM [8–11] in which the dynamic AFM mode was used to control the tip-sample separation. By this technique, we have realized a high resolution of 50 nm or even less in illumination mode. However, as the aperture of the probe becomes smaller, the intensity of the emitted light by

* Corresponding author. Tel.: + 81 47 392 7880; Fax: + 81 47 392 7822, e-mail: nakajima@tk.sii.co.jp.

the aperture decreases. The contrast of this kind of near-field microscopy is not good. The utilization of the polarization effect is one of several methods for enhancing the contrast of imaging in optical microscopy despite the low light intensity emitted by the aperture.

Optical microscopy with controlled polarization is an important tool for magneto-optics, liquid crystal and photo-luminescence. In magneto-optics, particularly, there is a need to increase the capacity of erasable data storage media by increasing bit density. The read–write system and media for magneto-optical data storage has been technologically attractive and has been eagerly developed. Higher resolution and sensitivity is required to examine the magnetic domains and walls of ferromagnetic materials for microscopy.

Many methods to observe the magnetic domains have been proposed such as polarizing microscopy, Lorentz transmission electron microscopy [12], magnetic-force microscopy (MFM) [13], and spin-polarized scanning electron microscopy [14]. However, each of them has some disadvantages such as resolution, sensitivity, sample preparation, costly instruments, and quantitative results. For example, MFM has good resolution, but it is difficult to quantify the magnetic properties from the MFM signal. Lorentz microscopy has high resolution but requires a thin-film sample.

Through SNOM with controlled polarization of subwavelength source and/or detector of light, polarization contrast is obtained with high resolution and sensitivity for imaging. This technique has been used to observe the magnetic domains using the magneto-optical effect [5,6,15]. In this paper, we describe the properties of plane polarization light emitted by the aperture and demonstrate polarization contrast imaging of the magnetic domains with the Faraday effect by the SNOM/AFM.

2. Experimental setup

Fig. 1 shows a schematic diagram of the SNOM/AFM system for near-field imaging of polarization contrast in transmission mode. An optical-probe mounted on a bimorph is vibrated vertically against the sample at the resonant

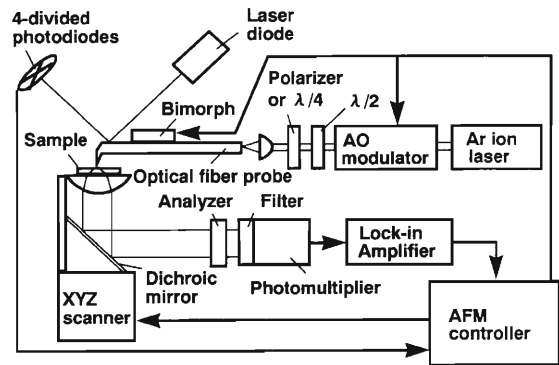


Fig. 1. Schematic diagram of the SNOM/AFM system for near-field imaging of polarization contrast in transmission mode.



Fig. 2. SEM image of optical fiber probe used in the SNOM/AFM system. The bending angle of the probe is about 80°.

frequency (typically 10–40 kHz). A laser beam reflected on a polished surface of the probe is detected and the change of the vibration amplitude of the probe is monitored. The vibration amplitude decreases as the tip of the probe approaches the sample surface, so that the tip–sample separation is controlled by maintaining the amplitude at a constant value in typical imaging. The vibration amplitude is in the range of 80–98% of the free vibration amplitude which is varied at 10–100 nm by the voltage applied to the bimorph. This makes it possible to change the interaction force between the probe and the sample.

Fig. 2 shows the SEM image of the optical fiber probe. To control the distance between the tip of

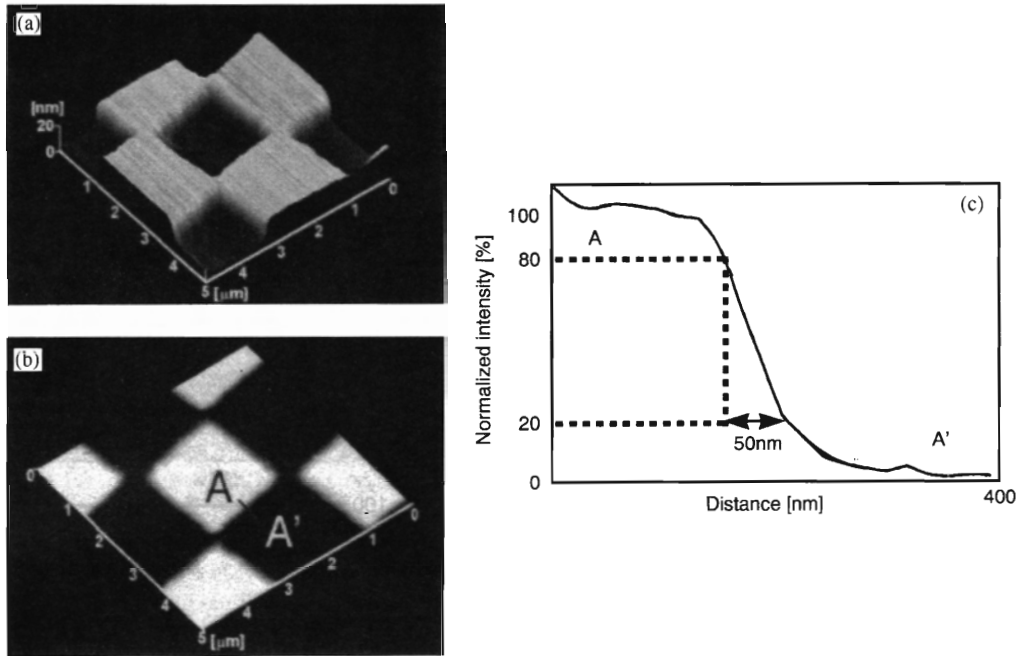


Fig. 3. SNOM/AFM images of 20 nm-thick chromium patterns on the quartz substrate: Topographical (a) and optical images (b). The scanned area is $5 \times 5 \mu\text{m}$.

the probe and the sample surface a single-mode optical fiber is sharpened and bent, so that it can be used as an AFM cantilever in the dynamic mode. The single-mode optical fiber whose core and cladding is 3.2 and 125 μm in diameter, respectively, is pulled to form the tip, and bent by the irradiation of a CO_2 laser. The bent angle is about 80° , and the point is 0.5 mm away from the apex of the tip. By coating the side of the tapered probe with 100–150 nm thick aluminum film, an aperture is fabricated at the apex of the probe. A 488 nm air-cooled argon ion laser with an out power 20–80 mW is used as the light source. The beam of the argon ion laser is modulated by an acousto-optic (AO) modulator to improve the S/N ratio of the optical signal, and coupled to a fiber at the other end of the probe. Half- and quarter-wave plates or polarizer are placed before the input fiber coupler. Because the optical fiber probe has retardation or perturbation properties, the desired polarization state of the input beam is produced by changing the orientation of the wave plates, and it makes it possible to control the polarization char-

acteristics of the light emitted by the aperture of the probe. After the light emitted by the probe transmits the sample, it is detected by a photomultiplier through a collimation lens, a dichroic mirror, an analyzer and an optical filter. The dichroic mirror is used to reduce the difference of the reflectance in the polarization direction of the incident light to the mirror. A particular transverse polarization component selected by the analyzer is measured in the far-field. The detected signal is amplified by a lock-in amplifier to reduce noise in the signal.

3. Results and discussion

3.1. Basic performance of SNOM/AFM

Fig. 3 shows topographic and near-field optical images of a 20 nm thick chromium film of $2 \times 2 \mu\text{m}^2$ test sample on a quartz substrate. The scanned area is $5 \times 5 \mu\text{m}^2$. The elevated parts in the topographic image (Fig. 3a) are the chromium patterns, which correspond to the dark areas in the

near-field optical image (Fig. 3b) because of the lower transmittance of the chromium film. Fig. 3c shows the optical profile which corresponds to the line in Fig. 3b. The width of the slope between the dark and bright part is about 50 nm on the 20–80% threshold. Because of the artifacts occurring in the near-field imaging, it is difficult to estimate the optical resolution and the aperture size by scanning across the topographical edge. However, the thickness of the chromium film is smaller than the slope width, and the enhancement of the optical intensity at the edge is small. Therefore, the aperture of the probe is roughly estimated to be 50 nm in diameter.

3.2. Polarization properties for the bending probe of an optical fiber

The polarization properties of the light emitted by the aperture was measured in the far-field. The relation between the rotation angle of the polarizer and the extinction ratio for the bent fiber with a cleaved end is shown in Fig. 4. When plane polarized light is coupled at the input end of the optical fiber, the light emitted by the core is normally elliptically polarized light because retardation caused by the anisotropy of the bent fiber, such as stress and deformation of the core, makes the fiber a quarter-wave plate. When the optical fiber is bent to about 80° of the bending angle, the light output from the optical fiber is normally elliptically polarized light. We can see that the plane polarized light which has a polarization extinction ratio of better than 100:1 is obtained from the optical fiber in Fig. 4. It is presumed that the extinction ratio of the bending fiber is improved by using an optical fiber with a small photo-elastic constant and inserting the compensation plate.

Fig. 5 is the relation between the extinction ratio of the light emitted by an aperture of the bent probe and rotation angle of a $\lambda/4$ plate. For examining polarization properties, we prepared a probe with aperture of 150 nm in diameter by the above-mentioned estimation method of the aperture size. When the retardation of the input light to the probe are adjusted adequately by rotating the $\lambda/4$ plates, the light emitted by an aperture of the tapered probe was observed to have a polarization extinction of better than 70:1 in Fig. 5. It was also

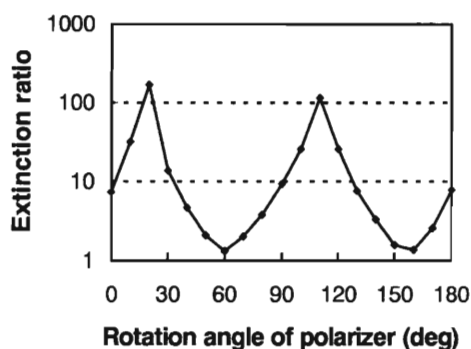


Fig. 4. Extinction ratio of light illuminated from the core of the bent optical fiber vs. the rotation angle of the polarizer.

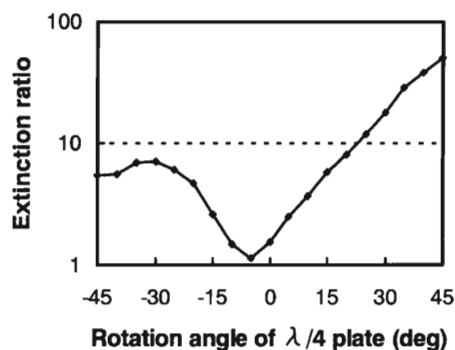


Fig. 5. Extinction ratio of light emitted by the aperture of the probe vs. the rotation angle of $\lambda/4$ plate.

observed that both the tapered and metal-coated probes exhibited depolarizing effects indicating we need to improve the quality of the tapered probe.

3.3. Polarization contrast of magneto-optical film with the Faraday effect

We confirmed the adaptability of SNOM/AFM for observing small magnetic domains of magneto-optical film with the Faraday effect. The sample was a 100 nm thick bismuth-substituted dysprosium-iron-garnet film on a glass substrate. The Faraday rotation angle of the sample was about 1.7° at the wavelength of 488 nm by means of the far-field optics. In the garnet film, bits with a size of about 3×1 and $0.7 \times 1 \mu\text{m}$ were written by a conventional magneto-optical read-write system using

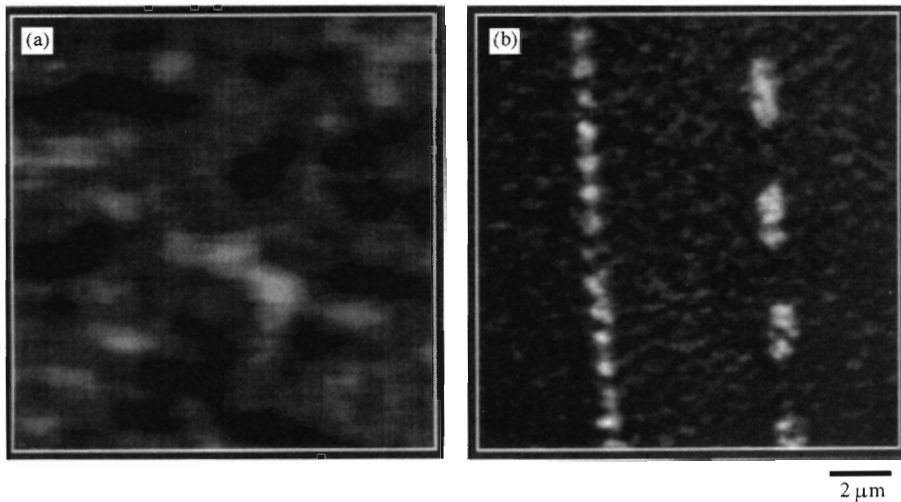


Fig. 6. Topographic (a) and polarization contrast images (b) of bits with a length of 0.7 and 3 μm in bismuth-substituted dysprosium-iron-garnet film with a thickness of 100 nm, which is observed by a SNOM/AFM.

a focused laser beam. The irradiation pulse width of the writing laser beam varies the bit length.

The small magnetic domains of the garnet film were observed by the SNOM/AFM system with plane polarized light emitted by the aperture. Fig. 6 shows the topographic (a) and the polarization contrast images (b) of bits written in the garnet film. The scanned area was $15 \times 15 \mu\text{m}^2$. The polarization contrast images have good contrast and the written bits can be clearly distinguished. We confirmed that the polarization contrast is lost and inverted by the change of the rotation angle of the analyzer. The different directions of rotation (clockwise or counterclockwise) which depend on the magnetization (up or down) of the garnet film, create the polarization contrast by detecting a particular polarization component in the light transmitted by the garnet film. Small bits with a length of 0.7 μm in the garnet film are clearly observed, and the resolution of the polarization contrast images is estimated to be beyond the diffraction limit of a conventional optical polarizing microscope.

4. Conclusions

We have demonstrated the applicability of the SNOM/AFM to image polarization contrast. The

bent probe used as the AFM cantilever shows retardation properties similar to a quarter-wave plate. However, control of the polarization properties of input light to the probe by wave plates allows the irradiated light from the aperture to have a polarization extinction ratio of better than 70 : 1. By detecting a selected polarization component in the transmitted light of the garnet film, we have indicated that SNOM/AFM imaging of perpendicularly magnetized domains is possible by using the polarization contrast caused by the Faraday effect.

Acknowledgements

This work was supported in part by a Grant-in-Aid from the Ministry of Education, Science and Culture. The authors wish to thank Dr. N. Kawamura (NHK science and Technical Res. Lab.) for supplying the garnet film.

References

- [1] A. Lewis, M. Isaacson, A. Harootunian, A. Muray, Ultramicroscopy 13 (1984) 227.
- [2] D.W. Pohl, W. Denk, M. Lanz, Appl. Phys. Lett. 44 (1984) 651.

- [3] E. Betzig, A. Harootunian, A. Lewis, M. Isaacson, *Appl. Opt.* 25 (1986) 1890.
- [4] E. Betzig, J.K. Trautman, T.D. Harris, J.S. Weiner, R.L. Kostelak, *Science* 251 (1991) 1468.
- [5] E. Betzig, J.K. Trautman, *Science* 257 (1992) 189.
- [6] E. Betzig, J.K. Trautman, R. Wolfe, E.M. Gyorgy, P.L. Finn, M.H. Kryder, C.-H. Chang, *Appl. Phys. Lett.* 61 (1992) 142.
- [7] S. Shalom, K. Lieberman, A. Lewis, R. Cohen, *Rev. Sci. Instr.* 63 (1992) 4061.
- [8] M. Fujihira, H. Monobe, H. Muramatsu, T. Ataka, *Chem. Lett.* (1994) 657.
- [9] N. Chiba, H. Muramatsu, T. Ataka, M. Fujihira, *Jpn. J. Appl. Phys.* 34 (1995) 321.
- [10] H. Muramatsu, N. Chiba, K. Homma, K. Nakajima, T. Ataka, S. Ohta, A. Kusumi, M. Fujihira, *Appl. Phys. Lett.* 66 (1995) 3245.
- [11] K. Nakajima, Y. Mitsuoka, N. Chiba, H. Muramatsu, T. Ataka, M. Fujihira, *SPIE* 2535 (1995) 16.
- [12] J.N. Chapman, A.B. Johnston, L.J. Heyderman, *J. Appl. Phys.* 76 (1995) 5349.
- [13] D. Rugar, H.J. Maimin, P. Guethner, S.E. Lambert, J.E. Stern, I. McFadyen, T. Yogi, *J. Appl. Phys.* 68 (1990) 1169.
- [14] K. Koike, K. Hayakawa, *Jpn. J. Appl. Phys.* 23 (1984) L187.
- [15] T.J. Silva, S. Schultz, D. Weller, *Appl. Phys. Lett.* 65 (1994) 658.